

Modeling of tunnel junctions for high efficiency solar cells

John R. Hauser,^{a)} Zach Carlin, and S. M. Bedair

Department of Electrical and Computer Engineering, North Carolina State University, Raleigh, North Carolina 27695, USA

(Received 10 June 2010; accepted 7 July 2010; published online 29 July 2010)

Ultrahigh efficiency, in the range of 40%, can be achieved in multijunction solar cells operating at high solar concentrations, larger than 100 suns. Critical to this approach are high band gap tunnel junctions that serve as electrically low loss interconnections between the cells. The purpose of this work is to theoretically model such wide band gap tunnel junctions and to explore the advantages of a staggered band line up for improving the peak tunnel current. Theoretical results are calculated for heterojunction diodes made of n^+ -InGaP/ p^+ -AlGaAs over a range of doping levels. The results illustrate the advantage of a conduction band discontinuity in achieving low interconnect resistance for multijunction solar cells. © 2010 American Institute of Physics. [doi:10.1063/1.3469942]

The highest conversion efficiency of solar cells has been achieved in stacked multijunction cells with three collecting cells of different band gaps. Recent progress based on three junction cells using GaInP (1.9 eV band gap), GaAs (1.43 eV band gap), and Ge (0.67 eV band gap) have been reported with conversion efficiencies of $\sim 32\%$ at 1 sun and $\sim 40\%$ at 240 suns.^{1–3} For voltage addition from the stacked cells, a low resistance, optically transparent interconnect must be made between the stacked cells.^{4,5} For such interconnects, current must flow from an n-type semiconductor layer into a p-type semiconductor layer and tunnel junctions are the typical approach for joining the stacked solar cells. Such tunnel junctions should be able to operate up to 1000 suns, with current densities of about 20 A/cm². The most difficult connecting tunnel junction connects the top solar cell to the underlying solar cell and the connecting junction must be transparent to the wavelengths collected by the underlying cells. Doping levels approaching 10^{20} cm⁻³ on both sides of the junction are also required and the dopants should have low diffusion properties to minimize junction degradation during subsequent epitaxial processes.

The basic theory of pn junction tunneling was developed by Keldysh and Kane^{6,7} and the tunneling current density can be expressed as follows:

$$J = A \exp(-BE_b^{3/2}/E_F)(\bar{E}/2)D = A \exp(-BE_b^{1/2}qW)(\bar{E}/2)D,$$

where

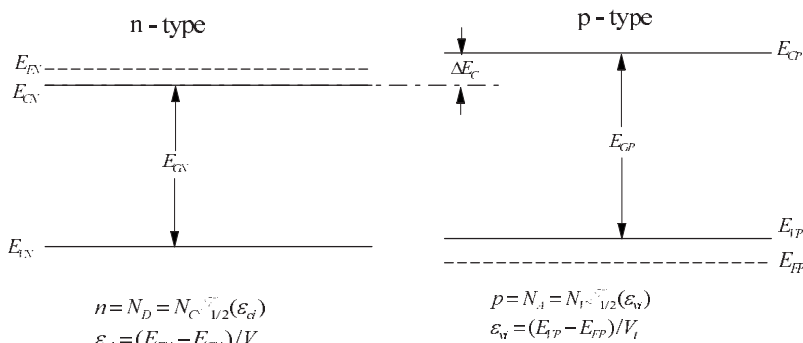


FIG. 1. Energy bands for tunneling junction model.

^{a)}Electronic mail: hauser@ncsu.edu.

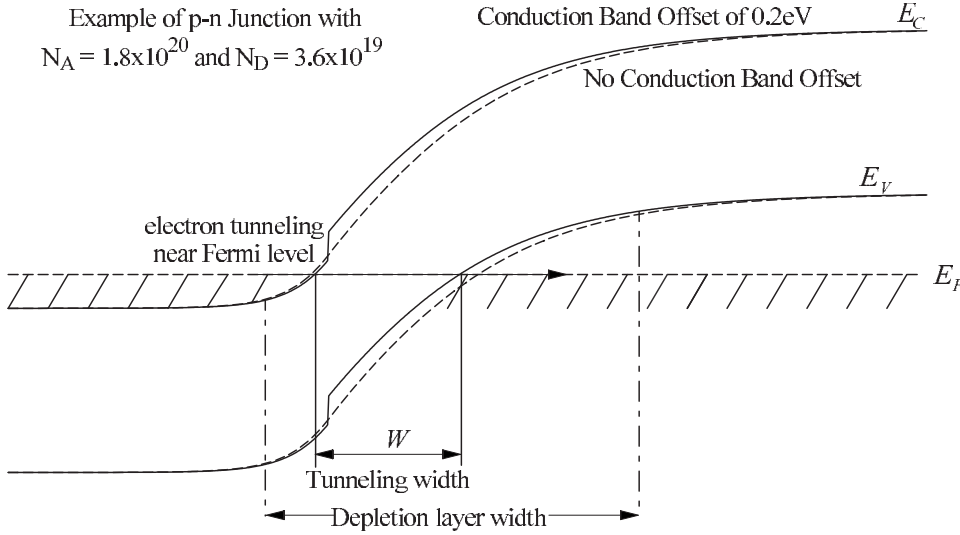


FIG. 2. Example of junction tunneling width and depletion layer width.

tentially have different band gaps (E_{GN} and E_{GP}). There may also be an intrinsic difference in the energy of the conduction band edges as shown in the figure (with ΔE_C). In the most general case, the electron and hole effective masses may differ on the sides of the junction as well as the dielectric constant. Heavy doping effects are also known to cause shifts in the conduction and valence band edges for heavily doped semiconductors resulting in a net reduction in the energy band gap. These are important in determining the locations of the intrinsic Fermi levels and consequently the junction built-in voltage. In this work, the heavy doping effects have been modeled as follows. For the majority carrier band edge (ΔE_{mj}), the shift has been modeled by the Coulomb energy around an impurity atom averaged over a spherical volume equal to the average volume occupied by an impurity atom. For the minority carrier bands, the contribution to band gap reduction (ΔE_{mn}) has been modeled by the reduced Coulomb energy around a minority carrier due to screening from the majority carriers.^{8,9}

These assumptions lead to the following expressions:

$$\Delta E_{mj} = \left(\frac{3q^2}{16\pi\epsilon} \right) \left(\frac{q^2 N}{\epsilon kT} \right)^{1/2} \quad \text{and} \quad \Delta E_{mn} = \left(\frac{q^2}{4\pi\epsilon} \right) \times \left(\frac{q\pi N}{2} \right)^{1/3}. \quad (2)$$

These heavy doping effects can be combined with the intrinsic band gaps and any intrinsic conduction band difference to evaluate the difference between the Fermi levels of the isolated semiconductors and this becomes the equilibrium built-in voltage across the tunneling junction. Figure 2 illustrates the resulting semiconductor band edges around the junction resulting from such a numerical calculation for a model tunneling junction with a band gap of 1.9 eV both with and without a conduction band edge difference. The tunneling width as well as the classical junction depletion layer width is shown in the figure for the conduction band offset calculation.

In many papers, tunneling width is approximated by the total width of the depletion layer.¹⁰ However, this overestimates the tunneling width and consequently will underestimate the tunneling current. For the particular example in Fig. 2, the tunneling width is about 42% of the classically calcu-

lated depletion layer width. Also it is seen that the tunneling width is reduced when a conduction band offset exists.

In order to verify the models discussed in the previous section, the theory has been applied to tunneling in GaAs diodes where the most extensive experimental data is available. The procedure was to numerically solve Poisson's equation for selected doping levels on each side of the junction from which the tunneling width can be extracted. This value was then used with Eq. (1) and the value of D then numerically calculated. Calculated peak tunneling currents for GaAs were found to be in very good agreement with previously reported data.¹⁰⁻¹³

With the GaAs results as model verification, the model has been applied to a wide band gap tunnel diode appropriate for use in the top cell of a three or four multijunction high efficiency solar cell. Potential materials for the tunnel junctions include $\text{Al}_x\text{Ga}_{1-x}\text{As}$ (with $x \sim 0.36$) and $\text{Ga}_x\text{In}_{1-x}\text{P}$ (with $x \sim 0.5$)^{2,5} with band gaps of around 1.9 eV. However, the doping density of n-type $\text{Al}_x\text{Ga}_{1-x}\text{As}$ has been found to be limited by DX center formation to the low 10^{18} cm^{-3} range. The model calculations have thus been based upon an $\text{n}+\text{Ga}_x\text{In}_{1-x}\text{P}$ and $\text{p}+\text{Al}_x\text{Ga}_{1-x}\text{As}$ diode with band gaps of 1.91 eV. Other parameters for the $\text{Ga}_x\text{In}_{1-x}\text{P}$ include $\epsilon_r = 11.75$, $m_c^* = 0.093m_0$, $m_{lh}^* = 0.14m_0$, and $m_{hh}^* = 0.60m_0$ and for the $\text{Al}_x\text{Ga}_{1-x}\text{As}$ include $\epsilon_r = 11.88$, $m_c^* = 0.093m_0$, $m_{lh}^* = 0.106m_0$, and $m_{hh}^* = 0.60m_0$.¹⁴⁻¹⁶

Experimental data indicates that although both materials have approximately the same energy band gap, the conduction band of the $\text{Ga}_x\text{In}_{1-x}\text{P}$ is lower than that of the $\text{Al}_x\text{Ga}_{1-x}\text{As}$ by a few tenths of an electronvolt. This is an important parameter with respect to the tunneling current. An example of such a conduction band offset is shown in Fig. 1. The conduction band offset has two effects: it lowers the tunneling barrier and reduces the tunneling width. Both of these are seen from Eq. (1) to increase the tunneling current.

Calculated peak tunneling currents for the model $\text{Ga}_x\text{In}_{1-x}\text{P}/\text{Al}_x\text{Ga}_{1-x}\text{As}$ tunnel junction are shown in Fig. 3 as a function of effective doping density $[N_A N_D / (N_A + N_D)]$. For a simple pn junction model, the depletion layer width is only a function of the effective doping density. However, because of the heavy doping effects of Eq. (2) the numerical results become a weak function of the individual doping densities as the three curves in Fig. 3 show for acceptor to donor

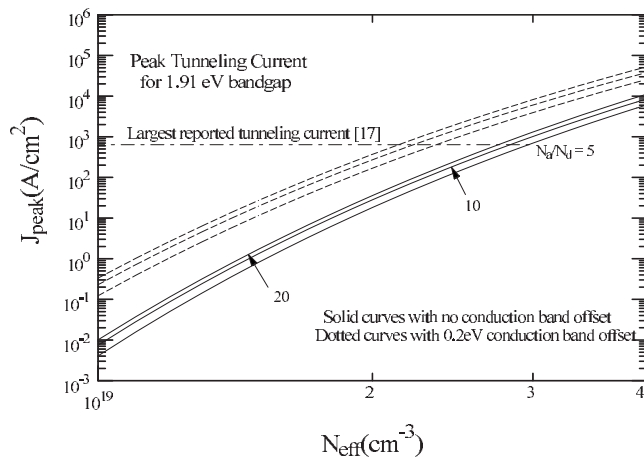


FIG. 3. Peak tunneling current for model 1.91 eV band gap tunneling junction.

doping ratios of 5, 10, and 20. The solid curves are for no conduction band offset and the dotted curves are for a 0.2 eV conduction band offset.

There is some uncertainty in the exact value of the conduction band offset. Direct measurements between $\text{Ga}_x\text{In}_{1-x}\text{P}$ and $\text{Al}_x\text{Ga}_{1-x}\text{As}$ are not available, so band offset values must be inferred from measurements between the constituent materials and GaAs. For $\text{Al}_x\text{Ga}_{1-x}\text{As}$ to GaAs, it is known that there is little difference in the valence bands and most of the energy band difference occurs in the conduction band. The measured valence band offset is $0.17x$ where x is the fraction of AlAs.¹⁷ Band offsets between GaAs and lattice matched GaInP are less certain with conduction band offsets ranging from 0.03 eV to as high as 0.39 eV.¹⁸ Measurements of internal photoemission by Haase *et al.*, have given a value of about 0.11 eV (Ref. 19) while a value of 0.24–0.25 eV is reported by Feng *et al.*¹⁸ From these two values, and the band gaps of the semiconductors, a conduction band offset between the $\text{Ga}_x\text{In}_{1-x}\text{P}$ and $\text{Al}_x\text{Ga}_{1-x}\text{As}$ layers lattice matched to GaAs of 0.29–0.15 eV is obtained. A somewhat mid point value of 0.2 eV has been used in the calculations here. Calculations for an $\text{Al}_x\text{Ga}_{1-x}\text{As}$ homojunction with the same band gap (1.91 eV) produce curves very close to those of Fig. 3.

More importantly than the peak tunneling currents is the current capability of the tunneling junction at low voltages. A common criterion is to look at the current capability at the thermal voltage of 0.025 V. These current values are shown in Fig. 4. Included in the figure are also current values needed for solar cells operating at 1, 10, 100, and 1000 suns. The short circuit current is approximately the same for two, three, or four junction solar cells. The largest reported peak tunneling current for a $\text{Ga}_x\text{In}_{1-x}\text{P}/\text{Al}_x\text{Ga}_{1-x}\text{As}$ tunneling junction is 637 A/cm^2 .²⁰ The effective doping density for this data has not been reported but the model indicates that this would require an effective doping density of around 2.5×10^{19} to 3.0×10^{19} . This is in the range of reported effective doping densities that have been achieved with the $\text{Ga}_x\text{In}_{1-x}\text{P}/\text{Al}_x\text{Ga}_{1-x}\text{As}$ junctions.⁵

Calculations have been performed for the expected tunneling currents of model $\text{Ga}_x\text{In}_{1-x}\text{P}/\text{Al}_x\text{Ga}_{1-x}\text{As}$ junctions that are lattice matched to GaAs (or Ge) and which are suitable for use in interconnecting the top two junctions in a high efficiency cascade solar cell structure. The calculations are

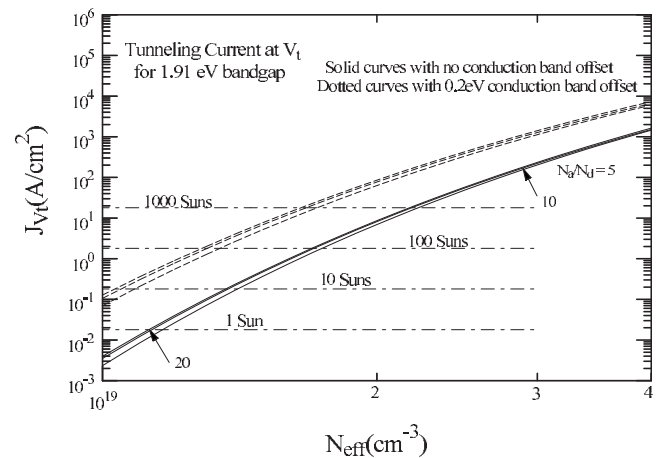


FIG. 4. Tunneling current at a voltage of V_t (0.026 V).

based upon the Kane theory of tunneling supplemented with a numerical solution of Poisson's equation to obtain the tunneling barrier and tunneling width. The calculations illustrate the importance of a conduction band offset between the $\text{Ga}_x\text{In}_{1-x}\text{P}$ and the $\text{Al}_x\text{Ga}_{1-x}\text{As}$. The offset is such as to enhance tunneling between an n-type $\text{Ga}_x\text{In}_{1-x}\text{P}$ and a p-type $\text{Al}_x\text{Ga}_{1-x}\text{As}$. The results indicate that the enhanced tunneling from the band offset can be as large as a factor of about 10.

- ¹J. M. Olson, S. R. Kurtz, A. E. Kibbler, and P. Faine, *Appl. Phys. Lett.* **56**, 623 (1990).
- ²R. R. King, D. C. Law, K. M. Edmondson, C. M. Fetzer, G. S. Kinsey, H. Yoon, R. A. Sherif, and N. H. Karam, *Appl. Phys. Lett.* **90**, 183516 (2007).
- ³R. R. King, R. A. Sherif, D. C. Law, J. T. Yen, M. Haddad, C. M. Fetzer, K. M. Edmondson, G. S. Kinsey, H. Yoon, M. Joshi, S. Mesropian, H. L. Cotal, D. D. Krut, J. H. Ermer, and N. H. Karam, European Photovoltaic Solar Energy Conference, Presented at the 21st European Photovoltaic Solar Energy Conference and Exhibition, Dresden, Germany, 4–8 September 2006.
- ⁴S. M. Bedair, M. F. Lamorte, and J. R. Hauser, *Appl. Phys. Lett.* **34**, 38 (1979).
- ⁵D. Jung, C. A. Parker, J. Ramdani, and S. M. Bedair, *J. Appl. Phys.* **74**, 2090 (1993).
- ⁶L. V. Keldysh, *Sov. Phys. JETP* **6**, 763 (1958).
- ⁷E. O. Kane, *J. Phys. Chem. Solids* **12**, 181 (1960).
- ⁸H. P. D. Lanyon and R. A. Tuft, *Tech. Dig. - Int. Electron Devices Meet.* **1978**, 316.
- ⁹S. S. Li, *Semiconductor Physical Electronics* (Plenum, New York, London, 1993), Chap. 5.
- ¹⁰L. Beji, B. El Jani, and P. Gibart, *Phys. Status Solidi A* **183**, 273 (2001).
- ¹¹L. L. Miller, S. W. Zeher, and J. S. Harris, *J. Appl. Phys.* **53**, 744 (1982).
- ¹²S. Ahmed, M. R. Melloch, E. S. Harmon, D. T. McIntuff, and J. M. Woodall, *Appl. Phys. Lett.* **71**, 3667 (1997).
- ¹³K. Zahraman, S. J. Taylor, B. Beaumont, J. C. Grenet, P. Gibart, and C. Verie, *Proceeding of 23rd IEEE Photovoltaic Specialist Conference*, Louisville, KY, 10–14 May 1993, p. 708.
- ¹⁴S. Adachi, *Properties of Semiconductor Alloys: Group-IV, III-V, and II-VI Semiconductors* (Wiley, New York, 2009).
- ¹⁵Y. Seko, S. Fukatsu, and Y. Shiraki, *J. Appl. Phys.* **76**, 1355 (1994).
- ¹⁶K. F. Brennan and P.-K. Chiang, *J. Appl. Phys.* **71**, 1055 (1992).
- ¹⁷A. J. Ekpunobi and A. O. E. Animalu, *Superlattices Microstruct.* **31**, 247 (2002).
- ¹⁸S. L. Feng, J. Krynick, V. Donchev, J. C. Bourgoin, M. De Forte-Poisson, C. Brylinski, S. Delage, H. Blanck, and S. Alaya, *Semicond. Sci. Technol.* **8**, 2092 (1993).
- ¹⁹M. A. Haase, M. J. Hafich, and G. Y. Robinson, *Appl. Phys. Lett.* **58**, 616 (1991).
- ²⁰R. R. King, C. M. Fetzer, P. C. Colter, K. M. Edmondson, J. H. Ermer, H. L. Cotal, H. Yoon, A. P. Stavrides, G. Kinsey, D. D. Krut, and N. H. Karam, 29th IEEE Photovoltaic Specialist Conference, New Orleans, 19–24 May 2002, p. 776.